Simultaneous photocharging and luminescence intermittency in silicon nanocrystals

2009 J. Phys.: Condens. Matter 21 235301

(http://iopscience.iop.org/0953-8984/21/23/235301)

J. Phys.: Condens. Matter **21** (2009) 235301 (8pp) doi:10.1088/0953-8984/21/23/235301

Simultaneous photocharging and luminescence intermittency in silicon nanocrystals

R J Rostron, Y Chao[1], G Roberts[2] and B R Horrocks[3]

School of Natural Sciences, Newcastle University, Newcastle upon Tyne NE1 7RU, UK

Received 19 December 2008, in final form 9 April 2009
Published 11 May 2009
Online at stacks.iop.org/JPhysCM/21/235301

Abstract

Contemporaneous measurements of the time dependence of photoluminescence and concomitant electrical conduction in films of alkylated silicon nanocrystals (NCs) during and between periods of continuous-wave laser irradiation of arbitrary duration establish the role played by photoionization to a conducting state in the intermittent light emission from silicon nanocrystals. The luminescence and current generated by electron photoejection both decay to non-zero, steady-state values during irradiation with visible laser light at incident intensities in the range 0.25–0.30 $\pm$ 0.01 kW cm^{-2}; on cessation of irradiation, the non-conducting photoluminescent state of the NCs is substantially regained. These observations are consistent with a model in which the decay of photoluminescence is ascribed to autoionization of the silicon NCs with a most probable lifetime $\langle T_a \rangle$, depending on particle size, and recovery of luminescence to electron–hole recombination characterized by a most probable lifetime $\langle T_{eh} \rangle$. Values of $\langle T_a \rangle = 1.08 \pm 0.03$ s and $\langle T_{eh} \rangle = 770 \pm 300$ s are extracted from nonlinear least-squares fitting to the time dependence of the photoluminescence intensity. The temporal behavior of the transient photocurrent is found to be quantitatively consistent with a one-dimensional model of diffusion of charge carriers between NCs. Integration of the time dependence of the photocurrent response coupled with an estimate of the volume irradiated with the laser light suggests ionization of one electron per NC during photon irradiation.

S Supplementary data are available from stacks.iop.org/JPhysCM/21/235301

(Some figures in this article are in colour only in the electronic version)

1. Introduction

Semiconductor nanocrystals exhibit a luminescence intermittency under continuous-wave irradiation whereby the light emitted by a single nanocrystal (NC) switches off and on in a random manner [1], the phenomenon being termed as 'blinking' [2]. Nanocrystals are much more stable against irreversible photochemical decomposition than single molecules and therefore provide systems in which to study this phenomenon over a wide range of conditions of irradiation intensity and time. The blinking of NCs is thought to result from photoionization of the illuminated particles to produce a charged NC core that does not emit light because of efficient energy transfer from photoexcited electron–hole pairs to the mobile charge carriers remaining in the core. Evidence for this conjecture is provided by observations of spectral diffusion [3] and electric force microscopy [4]. There has also been some discussion of where the charge resides [5, 6], and whether the photoexcited electrons can diffuse away from the original NC [7] or are trapped in surface states [8, 9]. The mechanism of the photoionization is thought to be an Auger process involving two excitons. However, there is not unanimous agreement on the dynamics of the blinking process [10, 11], and some workers [12] have noted that there can be a continuum of emissive states rather than a simple two-state 'on–off' situation [1]. Much work has focused on direct band-gap II–VI semiconductors, especially CdSe [12, 13]. As well as the fundamental interest in the physics of the process [10, 12–15], the intermittency of light emission

[1] Present address: School of Chemical Sciences and Pharmacy, University of East Anglia, Norwich NR4 7TJ, UK.
[2] Present address: School of Electrical, Electronic and Computer Engineering, Newcastle University, Newcastle upon Tyne NE1 7RU, UK.
[3] Present address: School of Chemistry, Newcastle University, Newcastle upon Tyne NE1 7RU, UK.

from CdSe NCs is of practical concern because it limits their application in the continuous monitoring of NC-labeled proteins and DNA molecules by confocal microscopy [13].

Silicon nanocrystals have recently been investigated for a number of reasons: Si has an indirect gap and there is evidence that the cause of intermittent light emission from Si-NCs is different to that of the direct-gap materials [6]. The intermittency of light emission from NCs brings about a reversible fading of photoluminescence when an ensemble of NCs is studied. The luminescence is typically collected in a confocal microscope where the stability of Si-NCs is a concern because they are susceptible to oxidation when exposed to high intensity laser irradiation. Alkylated Si-NCs prepared by a variety of methods [16, 17] are much less susceptible to oxidation because the *n*-alkyl organic monolayer passivates the particle surface and the Si–C bond anchoring the alkyl monolayer to the particle is chemically robust [17]. Oxidation of the alkylated Si-NCs employed in the experiments reported in this paper has previously been studied by photoemission spectroscopy, where it was observed that the particles were chemically stable except under prolonged irradiation with x-rays in the presence of water [18]. These factors enable us to study the time dependence of luminescence of Si-NCs over many minutes, to demonstrate that photofading is reversible and to detect directly the electrons ejected from the illuminated particles as a photocurrent.

This paper reports simultaneous measurements of photoluminescence fading and photoconduction of thin films of alkylated Si-NCs irradiated by continuous-wave (cw) laser light with the aim of mapping out the temporal correlation between light-emitting and charged states of the NCs. The proposed mechanism of luminous intermittency based on light absorption by Si-NCs followed by autoionization and charge–hole recombination is tested through concurrent measurements of photoluminescence and photoconduction in 12 μm-thick films over timescales of tens and hundreds of seconds. To the best of our knowledge, the present work represents the first experimental demonstration of the link between photoluminescence and electric conduction initiated by photoionization. The balance of the paper is made up as follows: experimental information on the optical and electrical measurements is given section 2 together with details of the preparation and characterization of Si-NCs; section 3 presents the results and their interpretation in terms of photoabsorption by Si-NCs followed by autoionization and electron–hole recombination; section 4 summarizes the work and draws conclusions from the experimental results.

2. Experimental details

In this section we describe the experiments undertaken to detect photoionization and luminescence of Si-NCs and briefly outline the methods of characterization of the NCs.

2.1. Detection of photoionization in alkyl Si-NCs

Figure 1 shows a diagram of the experimental arrangement employed to detect photoionization of 12 μm-thick films

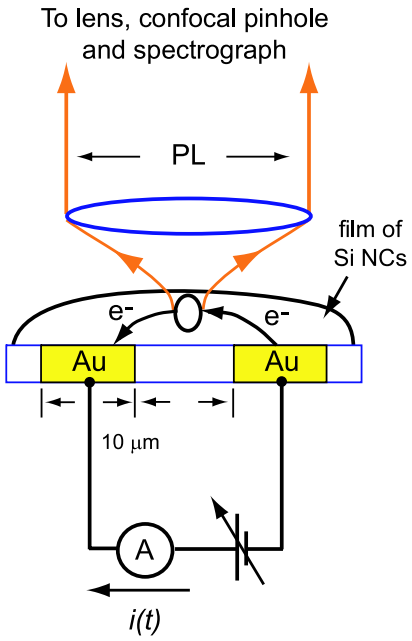

Figure 1. Schematic of the experiment: photoluminescence spectra $I(\lambda;t)$ and the photocurrent $i(t)$ generated by excitation of alkyl Si-NCs by laser light at $\lambda = 488$ (633) nm and an on-target intensity of 0.30 ± 0.01 (0.25 ± 0.01) kW cm^{-2} are measured simultaneously using a confocal microscope/spectrograph to irradiate and probe a film of nanocrystals covering a pair of in-laid gold microband electrodes. The focal point of the laser beam is at the mid-point of the film between the gold band electrodes. Predominantly orange luminescence from the Si-NC film was spectrally isolated using a monochromator with a bandwidth of 1 nm and detected by a CCD camera. In purely spectroscopic experiments, the Si-NCs were cast onto a glass microscope slide instead of microband electrodes.

of Si-NCs cast across two gold electrodes. The electrodes consisted of 4 gold microbands of width 10 μm separated by 10 μm on an SiO_2/Si substrate. Each electrode was individually addressable and the resistance of the intervening dielectric (oxide) was measured to be >200 GΩ. To excite luminescence, laser light at $\lambda = 488$ nm (Ar^+ laser) or 633 nm (HeNe laser) controlled by a manually operated shutter was focused at a point equidistant from each electrode of a neighboring pair and at a depth roughly midway through the film. Incident laser intensities at the sample surface were 0.25 ± 0.01 kW cm^{-2} at $\lambda = 633$ nm and 0.30 ± 0.01 kW cm^{-2} at $\lambda = 488$ nm. Simultaneous measurements of the induced photoluminescence and photocurrent were acquired by measuring the current flowing between the electrodes using an electrometer/voltage source controlled by a locally-written LabView^{TM} program.

2.2. Confocal photoluminescence measurements

A confocal microscope was used to record the temporal and spectral dependence of the intensity $I(\lambda;t)$ of photoluminescence emitted by Si-NCs subject to cw laser irradiation. Emitted light was transmitted through a Raman edge filter to remove the elastically scattered component and collected by a multimode optical fiber which served also as the confocal pinhole. The time dependence of $I(\lambda;t)$ was mapped out

at 0.1 s intervals for periods up to 5 min by detecting the luminescence at all wavelengths between 488 and 725 nm on a CCD camera. For spectral measurements, the filtered luminescence was resolved by a spectrograph equipped with a grating with 150 lines mm^{-1}, which provided a resolution of 0.5 nm, and detected by a CCD camera over a typical integration time of 0.1 s/pixel. For spectral imaging, a grating with 600 lines mm^{-1} was used coupled with detection over a typical integration time of 0.5 s/pixel. Each image was made up of 256 pixels × 256 pixels.

2.3. Preparation of alkyl Si-NC films

The preparation of the alkyl (11 carbon atoms) Si-NCs used in this work has been described elsewhere [19], a brief summary of which is provided in the supporting information (available at stacks.iop.org/JPhysCM/21/235301) which accompanies this paper. A thin film of the Si-NCs was drop-coated on to a glass microscope slide for measurements of photoluminescence or on to gold microband electrodes for detection of photoionization from a solution in dichloromethane (≃100 μg ml^{-1}) and dried in air. The thickness of the film was determined using a confocal microscope to observe the luminescence excited at $\lambda = 488$ nm as the focal point was scanned through the film. An example of a two-dimensional slice through such a film is shown in the supporting information (available at stacks.iop.org/JPhysCM/21/235301): this image shows the film is about 12 μm thick on average.

2.4. Characterization of alkyl Si-NCs

We have previously characterized the composition, structure and size of Si-NCs by photoemission, probe microscopy [18] and FTIR [20]. Absorption and emission spectra consistent with these measurements have also been reported [20–22]. A brief summary of those properties of the alkyl Si-NCs relevant to these investigations is as follows. FTIR and photoemission studies show that the particles are comprised of an Si core with a small, submonolayer amount of oxide and a capping alkyl monolayer, comprising undecyl $[-(CH_2)_{10}CH_3]$. X-ray powder patterns, Raman spectroscopy and high-resolution aberration-corrected transmission electron microscopy indicate that the Si core is crystalline with the same lattice parameters as the diamond structure of bulk Si [19]. The alkyl monolayer is chemically robust and bonded to the Si core via covalent Si–C bonds, not via the oxide. This monolayer stabilizes the nanocrystals against oxidation except under intense x-ray irradiation in the presence of water [18]. Vacuum ultraviolet photoexcitation spectra and optical luminescence generated by x-ray irradiation suggest that the orange emission monitored in the present experiments arises from excitation of unoxidized Si atoms [18, 21].

3. Results and discussion

The luminescence intermittency of semiconductor nanocrystals irradiated by low-intensity, cw light is generally interpreted in terms of photoionization of the optically accessible excited state $|1\rangle$, either by thermal or by Auger autoionization, to generate a charged state $|2\rangle$ which itself does not luminesce because of efficient non-radiative loss [1]: rather, $|2\rangle$ discharges when the separated electron–hole (e–h) pair created by autoionization recombines to re-generate either of the neutral states $|0\rangle$ or $|1\rangle$. Following the suggestion of Efros and Rosen [1], it is assumed here that charge neutralization of $|2\rangle$ results in $|1\rangle$, which subsequently undergoes fast vibrational relaxation to $|1'\rangle$. The bright state $|1'\rangle$ decays radiatively to $|0\rangle$ by emission of a photon at a wavelength longer than that of the initial $|1\rangle \leftarrow |0\rangle$ photoabsorption. The relevant photophysical processes are summarized by the scheme

$$|0\rangle + n\hbar\omega \overset{W}{\rightleftharpoons} |1\rangle \overset{T_a}{\rightarrow} |2\rangle \overset{T_{eh}}{\rightarrow} |1\rangle \qquad (1a)$$

$$|1\rangle \rightarrow |1'\rangle \overset{T_r}{\rightarrow} |0\rangle, \qquad (1b)$$

which is a simplified and amended version of the mechanism of random telegraphing proposed by Efros and Rosen [1]. Here, W denotes the rate of n-photon absorption and stimulated emission, T_a and T_{eh} are the characteristic decay times for autoionization and neutralization and T_r represents the radiative lifetime of the photoluminescent state $|1'\rangle$ generated by $|1\rangle$. Not included in equation (1), in contrast to the mechanism of [1], is further photoexcitation of $|2\rangle$ by the incident light because it is not expected to produce luminescence [6]. The rates of radiative decay and photon absorption at the intensities used in this work are five–six orders of magnitude larger than the rates $1/T_a$ and $1/T_{eh}$ of the ionization and re-neutralization processes of interest here. Previous studies of the radiative decay of excited states of Si-NCs have measured lifetimes on the order of microsecond [23] or shorter [24], while experiments in our group indicate that temporal relaxation of $|1\rangle$ of Si-NCs prepared by the method of section 2.3 is characterized by a distribution of lifetimes shorter than 25 μs [25]. In the experiments reported here, the luminescence decays under continuous-wave rather than pulsed irradiation: this work is not therefore concerned with the rate at which $|1'\rangle$ decays radiatively, but rather that at which the optically excited state $|1\rangle$ is lost by other processes such as electron transfer or photochemical reactions. We do not specify in equation (1*a*) how many photons are absorbed to reach the $|1\rangle$ state and leave open questions concerning the precise electronic structure of $|1\rangle$ and $|1'\rangle$.

A simple treatment of the rates of pair occupation of the NC states based on the mechanism of equation (1) can be made based on the premises that the applied light field rapidly establishes an equilibrium between $|0\rangle$ and $|1\rangle$, whose occupation probabilities are $P_0(t)$ and $P_1(t)$, and that autoionization and electron–hole recombination take relatively far longer by comparison. Likewise, vibrational relaxation of $|1\rangle$ to the emitting state $|1'\rangle$ is assumed to occur over a timescale much shorter than T_a, T_{eh} and T_r. The slow time rate of change of $P_1(t)$ is then

$$\frac{dP_1}{dt} = -\frac{P_1}{T_a} + \frac{P_2}{T_{eh}} \qquad (2)$$

with the assumption that $T_r \ll T_{eh}$, T_a. Setting $dP_1(t)/dt = 0$ in the limit $t \to \infty$, the ratio of neutral to charged NCs at steady state is then

$$\frac{P_0(t \to \infty)}{P_2(t \to \infty)} = \frac{T_a}{f[I(\lambda);\lambda]T_{eh}} = \frac{I_\infty}{I_0 - I_\infty}, \qquad (3)$$

where I_∞ and I_0 designate the PL intensity in the limits $t \to \infty$ and $t = 0$ respectively. In the limit $t \to \infty$, the fraction $f[I(\lambda);\lambda] = P_1(t \to \infty)/P_0(t \to \infty)$ is an increasing function of intensity $I(\lambda)$ and, for the Si-NCs studied here, and a decreasing function of wavelength between 488 and 725 nm. Under conditions of low-intensity irradiation such that saturation of the $|1\rangle \leftarrow |0\rangle$ transition is avoided, $f[I(\lambda);\lambda] \ll 1$ and $P_0(t)/P_2(t)$ is proportional to $P_{1'}(t)/P_2(t)$. Although it was not possible for us to make direct measurements of the value of $f[I(\lambda);\lambda]$ because of the difficulty of determining reliably the fraction of emitted light collected by the detection optics, the analysis of the experimental PL intensity in terms of equation (3) presented in section 3.1 indicates that $f[I(\lambda);\lambda]$ remains small at all times $0 \leqslant t \leqslant 300$ s; in the experiments reported in this paper, the condition $t \to \infty$ is reached about 200 s after $t = 0$. The authors of [1] used a sequence of random numbers to simulate the stochastic behavior of light emission from a single NC; here, we find that the kinetic approach leading to equation (3) suffices to account for the temporal dependence of luminescence from a macroscopic ensemble of NCs.

3.1. Fading and recovery of photoluminescence

Figure 2(a) shows the temporal behavior of the photoluminescence intensity $I(\lambda;t)$ from a film of alkyl Si-NCs. At a given incident laser power, the intensity of luminescence is greater under irradiation at 488 nm by an Ar ion laser than at 633 nm by a HeNe laser because the absorption coefficient of the Si-NCs increases at shorter wavelengths [20]. When the cw laser light is first incident on the NCs, a large initial PL intensity I_0 is observed which decays to a steady-state value I_∞ as $t \to \infty$: we found that an irradiation time of approximately 300 s was sufficient to reach steady state at $\lambda = 488$ nm and about 80 s at $\lambda = 633$ nm. The population of emissive NCs decays to an asymptotic limit when exposed to low-intensity cw light because the ratio $P_2(t)/P_1(t)$ of charged (dark) to neutral (bright) NCs increases until a steady state is reached where the rates of autoionization and electron–hole recombination are balanced. The decrease in PL intensity is more marked at the shorter wavelength where I_∞ reaches a level $I_\infty \simeq I_0/9$. However, after a recovery time of 10 or 60 s in the absence of irradiation, the PL intensity partially recovers when irradiation recommences. The recovery may be expressed as the fractional excess of the initial peak area compared to the steady-state value integrated over the following 300 s of irradiation, i.e. $\int_0^{300}[I(t) - I_\infty]/I_\infty \, dt$; this quantity is proportional to the fraction $P_{1'}(t)/P_0(t = 0)$ of particles in the uncharged, emissive state $|1'\rangle$ and could be determined more precisely than the value of intensity at any particular point in time. The extent of recovery increases as the time for charge neutralization is increased.

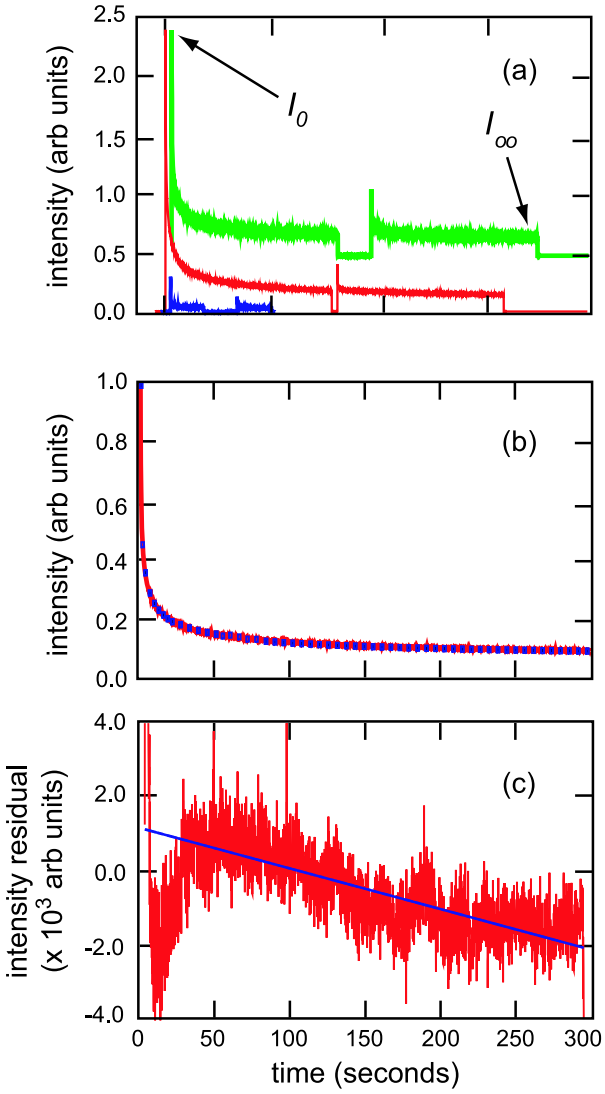

Figure 2. (a) Time-dependent luminescence showing the decay of intensity $I(\lambda;t)$ from a peak I_0 upon irradiation to a finite steady-state value I_∞ and partial recovery of intensity after a period during which the excitation source is extinguished. Middle line: $\lambda = 488$ nm excitation, 10 s recovery time. Upper line: $\lambda = 488$ nm excitation, 60 s recovery time. Lower line: $\lambda = 633$ nm excitation, 60 s recovery time. Relative to the middle curve, the upper and lower intensity traces are displaced in time by +25.0 s and the upper trace is displaced upwards in intensity by 0.5 arbitrary units for clarity. The incident laser intensities are given in the caption to figure 1. (b) Fit of $I(t)$ recorded at $\lambda = 488$ nm to equation (4): the data are shown as a line as in (a) and the fit as blue squares; for clarity, only every fiftieth fitted point is displayed. The most probable first-order decay time is $\langle\tau\rangle \simeq T_a = 1.08 \pm 0.03$ s, $\alpha_a = 4.07 \pm 0.04$ and the ratio of steady state to initial PL is $I_\infty/I_0 = 0.086 \pm 0.001$. The reduced chi-squared value of the fit is $\chi^2_r = 1.016$. (c) Plot of the intensity residuals $I(t) - I_{fit}(t)$ as a function of time with gradient 0.000 ± 0.002 s^{-1} and intercept $8.6 \pm 0.7 \times 10^{-4}$ arbitrary units.

Direct evidence that PL fading is caused by a physical process rather than a chemical reaction is provided by an examination of PL spectra at different times during the period of their decay. Figure 3 shows the spectral dependence of the luminescence shown in figure 2(a) at the onset of irradiation, after 90 s and after 300 s, when $I(\lambda;t)$ has nearly reached

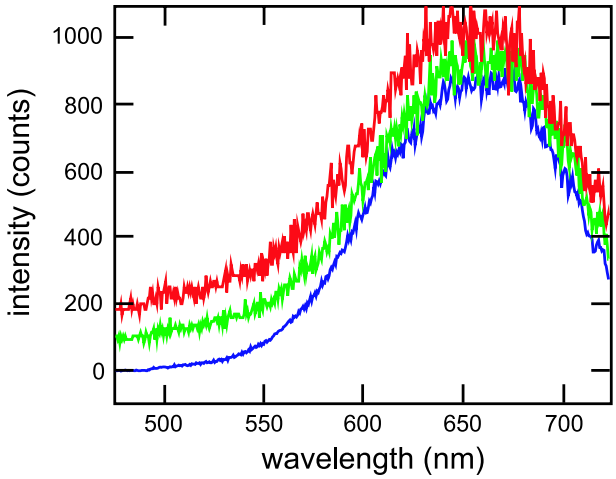

Figure 3. Photoluminescence spectra recorded 0 (lower), 90 (middle) and 300 (upper) s after the start of irradiation of alkyl Si-NCs by 0.30 ± 0.01 kW cm^{-2} light at $\lambda = 488$ nm. The spectra recorded at $t = 90$ and 300 s have been shifted upwards by 100 and 200 counts and multiplied by 11 and 17 respectively to facilitate comparison.

its steady-state limit. The spectra are essentially identical after normalization with respect to the peak intensities. This result is consistent with the interpretation that the asymptotic luminescence intensity is reached when a fraction of NCs cease to emit light, that in the absence of irreversible chemical changes, e.g. oxidation of charged NCs, luminescence spectra recorded at the start of irradiation ($t = 0$) and at steady state ($t \to \infty$) should be the same except for a scale factor, and that the intermittency should be reversible.

3.2. Dispersed kinetics of luminescence fading and recovery

The present analysis of data such as those displayed in figure 2(a) is based on the mechanism given by equation (1) with the interpretation that the characteristic decay times T_a and T_{eh} are randomly distributed about mean values due to the heterogeneity of NC size in the sample. It is possible to fit these curves by a sum of exponentials, but we prefer to interpret the time dependence of luminescence fading in terms of a single exponential with a single, characteristic decay time distributed about a most probable value for two reasons: first, this approach invokes fewer fitting parameters than even a double-exponential fit, whereas at least three exponentials are required to achieve a fit of comparable quality; and second, the physical significance of the lifetimes in such a tri-exponential fit is not so apparent [25, 26]. Following the procedure of [26], the slow decay of PL intensity may be written

$$I(t) = I_0 \int_0^\infty \phi(1/\tau)\exp[-t/\tau]\mathrm{d}(1/\tau), \qquad (4)$$

where $\phi(1/\tau)$ is a log-normal probability density function pertaining to a distribution of total decay rates characterized by a most probable value which varies as $\langle 1/\tau\rangle = (1/\tau)\exp[-\alpha\xi]$ with respect to a scaled (dimensionless) charging coordinate ξ whose probability density function is $(1/\sqrt{\pi})\exp[-\xi^2]$. Our analysis differs from that of [26] in one respect; we are considering the slow fading of luminescence of NCs under cw irradiation and therefore the luminescence intensity is proportional to the population of neutral particles. It is not unreasonable that there be a distribution of rates because there is a distribution of particle sizes [19] and the potential energy required to charge NCs depends inversely on their radius according to Gauss' law. Figure 2(b) displays a single-exponential fit to the data $I(t)$ shown in figure 2(a) obtained when the NCs are irradiated at $\lambda = 488$ nm, while figure 2(c) gives a measure of the quality of the fit via a plot of residuals $I(t) - I_{fit}(t)$. Except at very short times, where $|I(t) - I_{fit}(t)|$ increases to about 5.0×10^{-3}, equation (4) provides a reasonable fit to the time dependence of PL intensity. According to equations (2) and (4), the most probable first-order decay time extracted from the time-dependent photoluminescence data is $\langle\tau\rangle = \langle 1/T_a + 1/f[I(\lambda);\lambda]T_{eh}\rangle^{-1}$. However, we may approximate $\langle\tau\rangle$ as $\langle T_a\rangle$ because $\langle T_a\rangle \ll f[I(\lambda);\lambda]\langle T_{eh}\rangle$ (see below). Values of the parameters extracted from the fit given in figure 2(b) are $\langle T_a\rangle = 1.08 \pm 0.03$ s and[4] $I_\infty/I_0 = 0.086 \pm 0.001$. A large dispersion parameter $\alpha_a = 4.07 \pm 0.04$ was obtained from the fit, but this is anticipated by the dependence of the electrostatic contribution to the activation energy on particle size. It may be concluded that the simple reaction scheme of equation (1) provides a satisfactory description of the PL fading process, but that the time constant for autoionization should be treated as a random variable with a distribution determined by variations in particle size and local environment throughout the sample.

If a sample of Si-NCs is irradiated until the PL reaches a steady state, the majority of the particles at the focal point of the microscope will be charged if $\langle T_{eh}\rangle \gg \langle T_a\rangle$. In the absence of laser light, the only process occurring is electron–hole recombination and the fraction of initial PL intensity recovered when laser irradiation is re-commenced for a further 5 min can be used to determine a value for the most probable lifetime $\langle T_{eh}\rangle$. Figure 4 shows the recovery of PL intensity following this procedure; from these data the first-order rise time for electron–hole recombination was determined as $\langle T_{eh}\rangle = 770 \pm 300$ s with a dispersion parameter $\alpha_{eh} = 4.7 \pm 0.6$ and the fraction of luminescence intensity regained by further laser irradiation is 0.85 ± 0.03. These data also indicate that the process responsible for PL fading is substantially reversible and therefore unlikely to be due to a photochemical process.

A quantitative estimate of the value of $f[I(\lambda);\lambda]$ and a check on the consistency of the analysis of figures 2(b) and 4 can be made by comparing the measured ratio $I_\infty/(I_0 - I_\infty)$ with equation (3) subject to a minor modification to take account of the distribution of decay times. If $1/T_a$ and $1/T_{eh}$ are distributed according to $\langle 1/T_a\rangle\exp[\alpha_a\xi]$ and $\langle 1/T_{eh}\rangle\exp[\alpha_{eh}\xi]$ respectively and it is assumed that the lifetimes are slower or faster than average for both processes and not slow for one and fast for the other, so that the common variable ξ may be employed to calculate the mean of their ratio, then equation (3) becomes

$$\frac{I_\infty}{I_0 - I_\infty} = \frac{\langle T_a\rangle}{f\langle T_{eh}\rangle}\exp[(\alpha_{eh} - \alpha_a)^2/4]. \qquad (5)$$

[4] All uncertainties quoted in this study represent $\pm 2\sigma$.

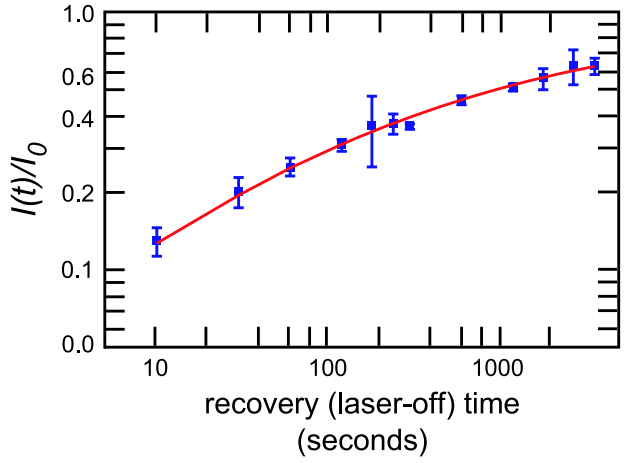

Figure 4. Fractional recovery of photoluminescence (squares with error bars) following a prior exposure time of 300 s and fit based on equation (4) (curve). The most probable first-order rise time describing the recovery of luminescence is $\langle T_{\rm eh}\rangle = 770 \pm 300$ s; the parameter describing the spread of the distribution is $\alpha_{\rm eh} = 4.7 \pm 0.6$; and the fraction of recovered luminescence intensity is $\int_0^{300}[I(t) - I_\infty]/I_\infty \, {\rm d}t = 0.85 \pm 0.03$.

Substituting values of $\langle T_{\rm a}\rangle$, $\langle T_{\rm eh}\rangle$, $\alpha_{\rm a}$ and $\alpha_{\rm eh}$ extracted from the fits to figures 2(b) and 4 we obtain $f[I(\lambda);\lambda] = 0.016 \pm 0.012$ and $(f[I(\lambda);\lambda]\langle T_{\rm eh}\rangle)^{-1} = 0.08 \pm 0.12$ s $^{-1}$. The error introduced by the assumption $\langle T_{\rm a}\rangle^{-1} \gg (f[I(\lambda);\lambda]\langle T_{\rm eh}\rangle)^{-1}$ in the analysis of the temporal behavior of PL such as is shown in figure 2(b) is therefore $8 \pm 12\%$ of the value of $\langle T_{\rm a}\rangle^{-1}$, which may be regarded as acceptable in view of the simplicity of the least-squares fitting procedure invoked to analyze the experimental data in terms of a single, log-normal distribution of decay times. We note that the value of $f[I(\lambda);\lambda]$ is subject to a large uncertainty, but also we do not require the value of this quantity for the physical interpretation of our results.

3.3. Detection of charging and current flow in alkyl Si-NCs.

Figure 5(a) shows the photocurrent $i(t)$ induced in a film of alkyl Si-NCs subject to laser irradiation for 60 s while figure 5(b) offers a comparison between the measured photocurrent and PL intensity. On irradiating the sample with laser light, $i(t)$ decreases from an initial maximum i_0 to reach a steady-state value i_∞. The difference $i_{\rm tr} = i_0 - i_\infty$ represents the transient current due to the start of laser irradiation. Another transient photocurrent $i_{\rm b}$ of opposite sign and approximately equal magnitude compared to $i_{\rm tr}$ was detected at the end of laser irradiation. The transient currents $i_{\rm tr}$ and $i_{\rm b}$ are due to charging and discharging of the Si-NCs, whereas i_∞ is a steady-state current which flows when the Si-NCs have acquired a quasi-constant net charge. This type of photocurrent–time behavior is characteristic of processes in which trap states become populated under irradiation [27]: the non-equilibrium carrier population decays after the light-off event and produces a photocurrent transient of opposite sign, but similar magnitude and lifetime to the light-on transient.

Figures 6(a) and (b) display the dependence of the total and steady-state photocurrents on the potential difference

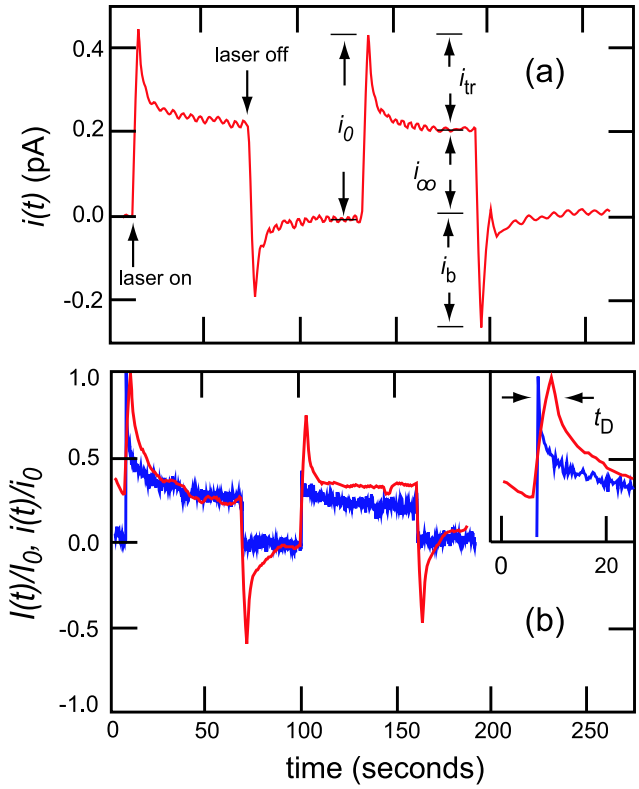

Figure 5. (a) Time dependence of the photocurrent $i(t)$ recorded on irradiation of alkyl Si-NCs at $\lambda = 488$ nm under the experimental conditions given in the caption to figure 1. The potential difference applied between the gold microband electrodes was 1.75 V. A dark current of 38 pA has been subtracted from $i(t)$ so that the trace shows directly the photon-induced current. Several aspects of the current–time traces discussed in the text are defined in the figure: the light-on transient component $i_{\rm tr}$; the steady-state photocurrent i_∞; the light-off transient current $i_{\rm b}$; and the peak photocurrent $i_0 = i_\infty + i_{\rm tr}$. (b) Correlation between photocurrent (dark curve) and PL (light curve) generated by laser light at $\lambda = 488$ nm in which both curves are arbitrarily scaled so that their maximum magnitudes are 1. The inset at top right of (b) shows the time delay $t_{\rm D}$ between the peak photocurrent and luminescence.

between the gold electrodes. Both i_0 and i_∞ exhibit ohmic behavior at potential differences up to about 2 V and saturation above. From the data recorded at potentials $\leqslant 3$ V a value of $q_{\rm tr} = 1.25 \pm 0.07$ pC is returned by integrating the transient currents following either light-on or light-off events for times sufficiently long so that $i_{\rm tr}$ has decayed to i_∞ and $i_{\rm b}$ has become the dark current. From this result we can estimate the number of electrons collected per NC by comparing the dimensions of the alkyl Si-NCs [19] with the dimensions of the irradiated volume. The irradiated volume is greater than the confocal volume because the electrons detected as photocurrent are not subject to the same optical restrictions as photons collected at the confocal pinhole. The irradiated volume was therefore estimated as that of the solid of revolution bounded by the hyperbolic variation of the diameter of a Gaussian light beam as far as the Rayleigh length along the direction of propagation either side of the minimum waist position. For an objective lens with a numerical aperture of 0.9 and assuming an index $n = 1$ within the sample, the irradiated volume is then

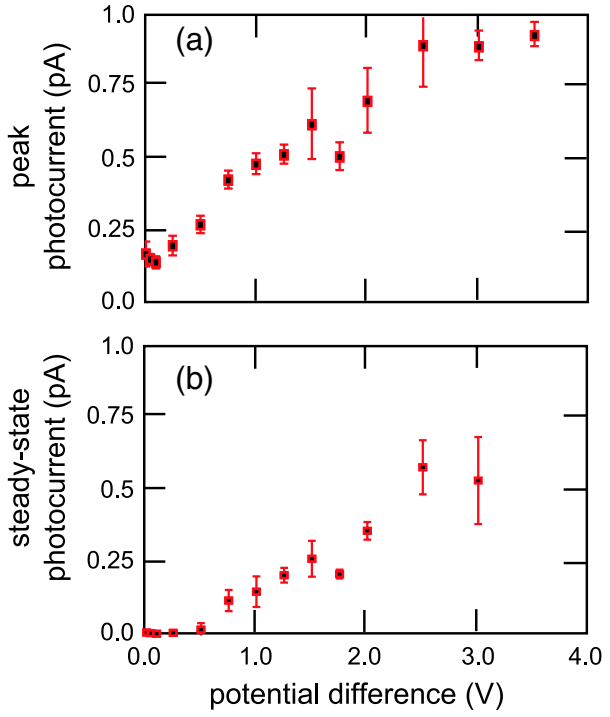

Figure 6. Graphs of photocurrent induced in alkyl Si-NCs by 488 nm laser light at an intensity 0.30 ± 0.01 kW cm^{-2} versus potential difference between electrodes as shown in the arrangement of figure 1: (a) peak photocurrent i_0 versus potential difference; (b) steady-state photocurrent i_∞ versus potential difference. The error bars represent the standard errors of $\pm 2\sigma$ about mean values obtained from four measurements.

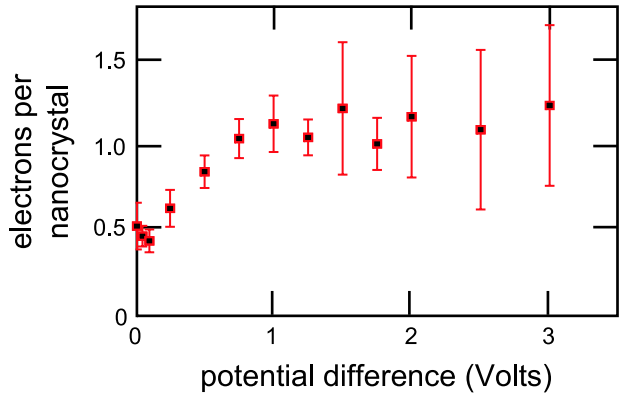

Figure 7. Number of electrons collected per particle in a film of alkyl Si-NCs within the focal volume irradiated by laser light at $\lambda = 488$ nm as shown in figure 1. The error bars represent standard errors of $\pm 2\sigma$ about mean values obtained from four repeated measurements.

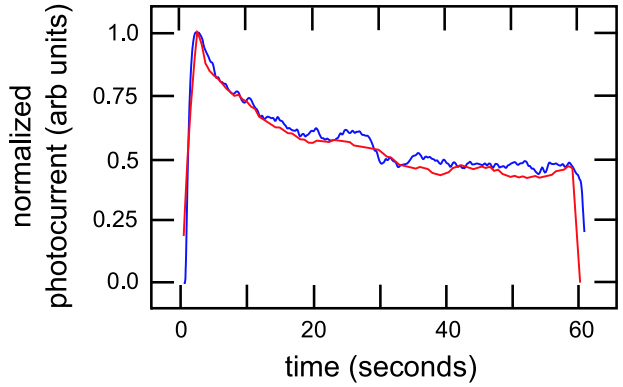

Figure 8. Measured (dark curve) and simulated (light curve) transient photocurrents with the peak of one normalized to that of the other. To perform the simulation, the integrated experimental PL transient of figure 2(b) obtained at $\lambda = 488$ nm, assumed to be directly proportional to the number of electrons, was used as input to a one-dimensional diffusion problem in which the evolution of the electron density field in the Si-NC film was obtained by integration of Fick's second law over a distance of 8 μm using an explicit finite difference algorithm with temporal and spatial discretizations of 0.02 s and 0.8 μm and a diffusion coefficient of $D = 10^{-7}$ cm^2 s^{-1}.

0.35 μm^3. With the assumption that Si-NCs adopt a close-packing arrangement such that they occupy about 0.74 of the irradiated volume, the number of Si-NCs of diameter 5 nm in the irradiated volume is 7.9×10^6; if each NC were to transfer a single electron, the total charge collected would then be about 1.27 pC. Figure 7 indicates the number of electrons transferred per Si-NC subject to potential differences up to 3 V. The close agreement between calculated and measured values of q_{tr} is somewhat fortuitous given the size of the error bars associated with the individual data points in figure 7 and the approximations employed. It can be concluded, however, that approximately one electron is collected per particle: this result seems reasonable because, on the one hand a significant electrostatic barrier would be expected for the transfer of a second electron, and on the other, the reduction in PL intensity would not be so marked as observed if less than a single electron were transferred per particle.

The detection of a photocurrent due to charging of the NCs relies on charge transport through the film of alkyl Si-NCs. An estimate of the transport rate and some insight into the mechanism of transport can be obtained from a direct comparison of the time dependence of PL and the photocurrent shown in figure 5(b). The comparison reveals that maximum PL intensity is reached less than 1 s after the laser irradiates the NC film, with a subsequent delay of $t_D = 2.1 \pm 0.1$ s before the peak in the photocurrent occurs (see inset to figure 5(b)). This is analogous to electrochemical time-of-flight experiments in which the diffusion of a pulse of charged molecules produced at one electrode (in our case the focus of the laser) is monitored by observing the peak in current at a collector electrode [28]. The delay time t_D is given by a form of the Smoluchowski equation $t_D = d^2/DK^2$, where d is the distance traveled, D the effective diffusion coefficient and K depends on the experimental geometry. The transient photocurrent may be modeled as a one-dimensional diffusion problem in which the geometry of the experimental set-up shown in figure 1 is approximated by a single spatial coordinate and the PL signal is used to provide the boundary condition at the source, i.e. to allow the assumption that the charge generated by irradiation is proportional to the observed PL intensity as a function of time. It is also presumed for simplicity that electrons arriving at the gold electrode are immediately transferred to the external circuit, i.e. that the kinetics at the NC/Au interface are transport controlled. Figure 8 compares the photocurrent simulated in

this way with the measured current of figure 5(a). The value $D = 10^{-7}$ cm^2 s^{-1} for the electronic diffusion coefficient used in the simulations is typical of electron hopping processes in polymer films and films of alkyl-capped gold NCs [29]. Since we do not know the quantum yield of luminescence, we cannot model the amplitude of the photocurrent peak, only the time at which it occurs. Nevertheless, the agreement between the measured current and that computed by solving the diffusion equation for the transport of electrons through the NC films permits the conclusions that the mechanism of charge transport is likely to involve electrons hopping between neighboring NCs and that the process can be described moderately well by a one-dimensional diffusion equation.

4. Conclusions

The fading of luminescence of a film of alkyl-capped Si nanocrystals subject to cw irradiation by laser light at $\lambda = 488$ or 633 nm is found to be essentially entirely reversible over timescales up to 5 min, which suggests that suppression and recovery of luminescence be due to an electron transfer process rather than an irreversible chemical change. The intermittency of luminescence can be described by a sequence of photoabsorption, autoionization and electron–hole recombination steps, which is a simplified version of the model presented by Efros and Rosen [1]. Most probable lifetimes of $\langle T_a \rangle = 1.08 \pm 0.03$ s and $\langle T_{eh} \rangle = 770 \pm 300$ s are determined for autoionization of Si-NC excited states and electron–hole recombination respectively when allowance is made for a log-normal distribution of decay times due to a distribution of particle sizes and compositions. The time dependence of the photocurrent detected at gold microband electrodes inserted in the Si-NC film provides a quantitative corroborant to the interpretation of the temporal behavior of photoluminescence. A limiting value of approximately one ejected electron per particle irradiated is collected at high applied potentials on the assumption of Gaussian ray optics. The delay between the rise of the luminescence intensity and of the photocurrent is consistent with diffusion of electrons in the film of nanocrystals with an effective diffusion coefficient of $D = 10^{-7}$ cm^2 s^{-1}.

Acknowledgments

We are grateful for support of this work by EPSRC though grant GR/S48240/01 and the UK Regional Development Agency *One North East*. RJR thanks the RDA for a research studentship.

References

[1] Efros A L and Rosen M 1997 *Phys. Rev. Lett.* **78** 1110
[2] Nirmal M *et al* 1996 *Nature* **383** 802
[3] Neuhauser R G *et al* 2000 *Phys. Rev. Lett.* **85** 3301
[4] Kruass T D and Brus L E 1999 *Phys. Rev. Lett.* **83** 4840
Krauss T D, O'Brien S and Brus L E 2001 *J. Phys. Chem.* B **105** 1725
[5] Rodríguez-Viejo J, Mattoussi H, Heine J R and Kuno M K 2000 *J. Appl. Phys.* **87** 8526
Wang X, Qu L, Zhang J, Peng X and Xiao M 2003 *Nano Lett.* **3** 1103
[6] Cichos F, Martin J and von Borczyskowski C 2004 *Phys. Rev.* B **70** 115314
[7] Sychugov I, Juhasz R, Linnros J and Valenta J 2005 *Phys. Rev.* B **71** 115331
[8] Heyes C D, Kobitski A Yu, Breus V V and Nienhaus G U 2007 *Phys. Rev.* B **75** 125431
[9] Stefani F D, Knoll W, Kreiter M, Zhong X and Han M Y 2005 *Phys. Rev.* B **72** 125304
[10] Tang J and Marcus R A 2005 *Phys. Rev. Lett.* **95** 107401
Tang J and Marcus R A 2005 *J. Chem. Phys.* **123** 054704
[11] Sher P H *et al* 2008 *Appl. Phys. Lett.* **92** 101111
[12] Banin U *et al* 2006 *Nano Lett.* **6** 843
[13] Biju V *et al* 2005 *J. Phys. Chem.* B **109** 14350
[14] Cakir R, Grigolini P and Krokhin A A 2006 *Phys. Rev.* E **74** 021108
[15] Frantsuzov P A and Marcus R A 2005 *Phys. Rev.* B **72** 155321
[16] Sweryda-Krawiec B, Cassagneua T and Fendler J H 1999 *J. Phys. Chem.* B **103** 9524
Nayfeh M H *et al* 2001 *Appl. Phys. Lett.* **78** 1131
Holmes J D *et al* 2001 *J. Am. Chem. Soc.* **123** 3748
Ding Z F *et al* 2002 *Science* **296** 1293
Li Z F and Ruckenstein E 2004 *Nano Lett.* **4** 1463
Hoshino A, Yamamoto K, Warner J H and Tilley R D 2005 *Angew. Chem.* **44** 4550
[17] Li X G, He Y Q and Swihart M T 2004 *Langmuir* **20** 4720
Hua F J, Erogbogbo F, Swihart M T and Ruckenstein E 2006 *Langmuir* **22** 4363
[18] Chao Y *et al* 2005 *J. Appl. Phys.* **98** 044316
[19] Chao Y *et al* 2007 *Nat. Nanotechnol.* **2** 486
[20] Lie L H *et al* 2002 *J. Electroanal. Chem.* **538** 183
[21] Chao Y *et al* 2006 *Appl. Phys. Lett.* **88** 263119
[22] Lie L H *et al* 2004 *Faraday Discuss.* **125** 235
[23] Credo G M, Mason M D and Buratto S K 1999 *Appl. Phys. Lett.* **74** 1978
Linnros J, Lalic N, Galeckas A and Grivickas V 1999 *J. Appl. Phys.* **86** 6128
[24] English D S *et al* 2002 *Nano Lett.* **2** 681
[25] Rostron R J, Horrocks B R and Roberts G 2009 *J. Appl. Phys.* **105** 094302
[26] van Driel A F *et al* 2007 *Phys. Rev.* B **75** 035329
Nikolaev I S *et al* 2007 *Phys. Rev.* **75** 115302
[27] Searson P C, Macdonald D D and Peter L M 1992 *J. Electrochem. Soc.* **139** 2538
[28] Amatore C, Sella C and Thouin L 2006 *J. Electroanal. Chem.* **593** 194
[29] Wuelfing W P *et al* 2000 *J. Am. Chem. Soc.* **122** 11465
Mao F, Mano N and Heller A 2003 *J. Am. Chem. Soc.* **125** 4951